ISSN 0010-5082, Combustion, Explosion, and Shock Waves, 2021, Vol. 57, No. 2, pp. 222–231. © Pleiades Publishing, Ltd., 2021.
Russian Text © W. Xiao, K. Chen, M.-F. Yang, X.-W. Hong, H.-W. Li, B.-L. Wang.

Effects of the Particle Size and Gas Environment on Afterburning Reactions and Explosion Performance of Aluminized HMX-Based Explosives

W. Xiao[a], K. Chen[a], M.-F. Yang[a], X.-W. Hong[b], H.-W. Li[a], and B.-L. Wang[a]

UDC 534.222.2

Published in *Fizika Goreniya i Vzryva*, Vol. 57, No. 2, pp. 104–115, March–April, 2021.
Original article submitted November 29, 2019; revision submitted May 15, 2020; accepted for publication June 1, 2020.

Abstract: In this paper, confined explosions of HMX-based aluminized explosives in a spherical chamber are studied. The effects of aluminum particles on the afterburning reaction and explosive performance are obtained by changing the size of the particles and the gas environment. The results show that the concentration of oxygen in air is not sufficient to support complete combustion of aluminum particles. The estimated oxidation rate of aluminum particles is 87–93%, and it tends to decrease with increasing particle size. Part of aluminum particles oxidize with detonation products, and the reaction can last for hundreds of microseconds. However, the degree of oxidation between the large-sized aluminum particles and detonation products is small. A new method is used to estimate the initial energy of detonation by observing the time difference between sensing the initial light and the pressure wave. This method leads to a conclusion that some of the aluminum particles are oxidized during detonation and provide additional energy to the primary blast wave. Small micron-sized aluminum particles in the range of 48.9 nm to 46.7 μm extend the duration of the fireball.

Keywords: aluminized explosive, afterburning reaction, confined explosion, aluminum particle.

DOI: 10.1134/S0010508221020118

INTRODUCTION

Damage of a target by an aluminized explosive depends on the pressure and thermal effects of the explosion. The initial energy is mainly from the detonation reaction, and the subsequent high pressure and high temperature are derived from the extra energy generated by afterburning reactions of the aluminum particles [1–3]. However, the size of the aluminum particles affects the afterburning reaction. Therefore, it is essential to optimize the aluminum particle size to increase the energy release efficiency of the aluminized explosive.

At present, there are many studies on the afterburning reactions of aluminized explosives [4]. Previous studies [5] showed that aluminum particles begin to react after approximately 5–100 μs after detonation. This phenomenon may be related to a dense oxide film (Al_2O_3) on the surface of the aluminum particles. The high decomposition temperature of this oxide film hinders the combustion of aluminum particles. When the explosion begins, the activated aluminum expands behind the Chapman–Jouguet (CJ) surface due to a rapid increase in temperature. Thereafter, the oxidized shell of the surface is broken so that the aluminum particles come into contact with oxygen. However, some studies [6, 7] showed that the way in which activated aluminum breaks through the oxide shell is also likely to

[a]School of Chemical Engineering, Nanjing University of Science and Technology, Nanjing, 210094 China; boliangwang@163.com; iridescent_bubbles@163.com.
[b]School of Mechanical Engineering, Nanjing University of Science and Technology, Nanjing, 210094 China.

be a phase transition of Al_2O_3. Finally, the released active aluminum rapidly reacts with the surrounding detonation products and oxygen to form Al_2O_3.

Regarding the effect of aluminum particles on the explosive properties, Peuker et al. [8] found that an early reaction of aluminum enhanced the primary explosive blast, and this reaction was approximately half aerobic and half anaerobic. However, in the particle size range of 3–40 μm, the effect of the aluminum particle size on the explosive performance was negligible. In addition, the results also showed that the fraction of oxygen in air was sufficient to oxidize aluminum particles within 10 μm. Lewis et al. [9] observed that aluminum particles emit light at the late stage of the explosion, while the intensity and duration of the luminescence depend on the size of the aluminum particles. They believed that the afterburning reaction had experienced multiple stages in the evolution of the fireball.

Tanguay et al. [10] speculated that the convective effect of the explosion field led to a decrease in the dependence of the aluminum particle size on the oxidation rate. Small particles react in a kinetic manner rather than in a diffusion manner because the mass diffusion coefficient was very large due to their small size. Therefore, there was always enough oxidant available for aluminum particles, and the ultimate rate limiter was that of chemical kinetics [11]. Park et al. [12] determined that aluminum particles have a burning rate limited by diffusion of particles if the particle size is larger than 20 μm. If the particle size is smaller than 10 μm, the burning rate is limited in dynamics. The research of Tanguay et al. [10] also showed that aluminum particles of 10 μm and smaller are no longer burned in the gas-phase diffusion flame, while the burning time of nano-sized particles is significantly dependent on pressure and temperature. McNesby et al. [2] found that the combustion reaction of smaller aluminum particles stopped faster. The reason may be that the aluminum particles were not thrown by the blast wave into the reactant mixture layer, even within the blast wave range. However, large aluminum particles were more likely to be propelled into the oxygen-rich gas environment, resulting in a stronger afterburning reaction. Trzciński [13] believed that a large specific surface area facilitated the heat exchange and oxidation reactivity of aluminum particles with detonation products and air. Moreover, the extra heat released by the reaction of small-sized aluminum particles with oxygen or detonation products increased the temperature of the explosive product, which, in turn, increased the pressure in the combustion chamber. The data of Maiz et al. [14] showed that the temperature of the fireball containing large-sized particles was 200 K higher than that of small-sized aluminum particles. In the case of a layered charge, this difference was very small.

The current research on the afterburning reaction in HMX-based aluminized explosives is limited. Moreover, the quality of the charges in the confined explosion was rather low, which was not conducive to the complete release of the energy in the aluminized explosive. In this study, confined explosion tests were carried out in a 1.43-m^3 spherical chamber with different atmospheres. The afterburning reaction was studied by observing the duration of light emission, intensity of Al_2O_3 formation, and lifetime of the explosion fireball. In addition, the time difference between sensing the initial light and pressure wave arrival was used as a new method to estimate the initial energy of the explosion. The overpressure and total impulse were also used to study the effect of the aluminum particle size on the explosion performance. The research described in this paper can provide a reference for the designing formulations of aluminized explosives to enhance the afterburning effect and the damage effect.

EXPERIMENTS

Four kinds of aluminized explosives containing aluminum particles of different sizes were studied. The aluminum particles were all spherical, and their size and specific surface area were measured by an ultrahigh-speed intelligent laser particle size analyzer. Besides, the contents of active aluminum were also obtained by the method of chemical solution titration (conversion of Fe^{3+} and Fe^{2+}) [15]. The mixtures consisted of HMX, aluminum particles, and a binder. Their formulations and the parameters of the aluminum particles are summarized in Table 1. Surprisingly, the results in Table 1 show that over 30% of the aluminum powder (48.9 nm) from the new packaging has been oxidized. This means that the activity of nano-aluminum should be considered in the present study. The specific surface area of the particles increased as the particle size decreased, which was expected. The mixtures were produced using the "wet method" [16–17]. The topographical features were observed by scanning electron microscopy (SEM), and the SEM images of the aluminized explosive granules are shown in Fig. 1.

As shown in Fig. 1, the surface of HMX particles with an angular shape adhered to the aluminum particles. It was obvious that the mixtures of TBX-A1 and TBX-A2 had a neat and smooth surface. The other two samples were rugged and rough. It should be noted that the alignment of the aluminum particles was also a more serious manifestation of their agglomeration.

Table 1. Composition of aluminized explosives and parameters of the aluminum particles

Name	Composition, %			Aluminum particles		
	HMX	Al	binder	median diameter	active aluminum, %	specific surface area, m^2/g
TBX-A1	59	33	8	48.9 nm	68.3	10.02
TBX-A2	59	33	8	5.4 μm	88.1	1.74
TBX-A3	59	33	8	23.8 μm	97.1	0.31
TBX-A4	59	33	8	46.7 μm	98.5	0.14

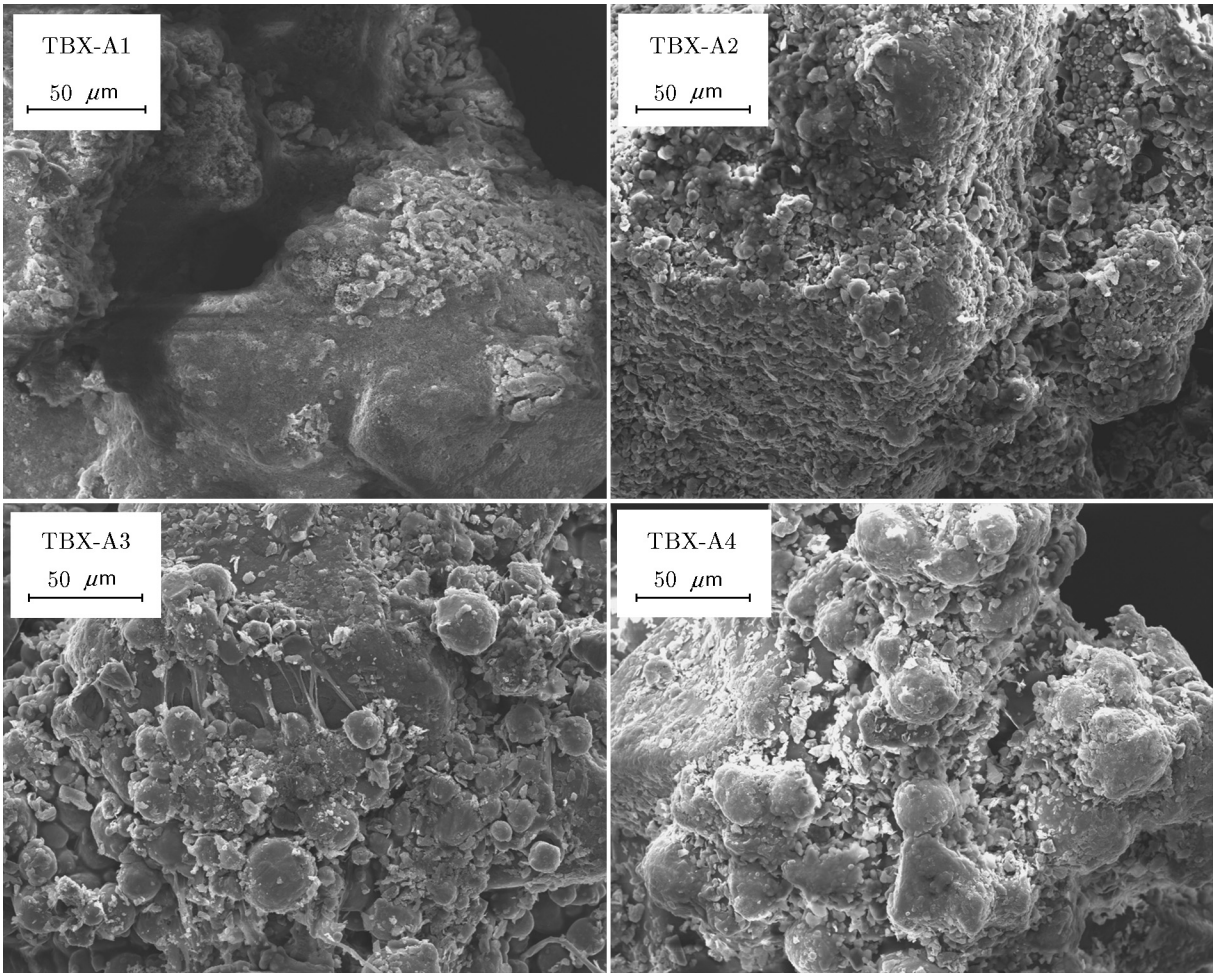

Fig. 1. SEM images of aluminized explosive granules.

Due to the effect of the van der Waals forces and Coulomb forces [18] coupled with a binder, small-sized aluminum particles could easily unite together. Agglomeration especially occurred for nanoscale aluminum particles, where this phenomenon was more pronounced than that at the micron scale. Large micron-sized aluminum particles, even under the action of a binder, were difficult to firmly bond to the surface of the HMX particles, in particular, in the case of TBX-A4, which looked as if many aluminum particles were piled up together and leaned onto a part of the HMX particles. The mixtures were pressed in the form of cylindrical charges, and each charge was 100 g. The charge had a diameter of 40 mm and a height of 40 mm. Before the test, charges were fixed with a booster (8 g) and an electric detonator.

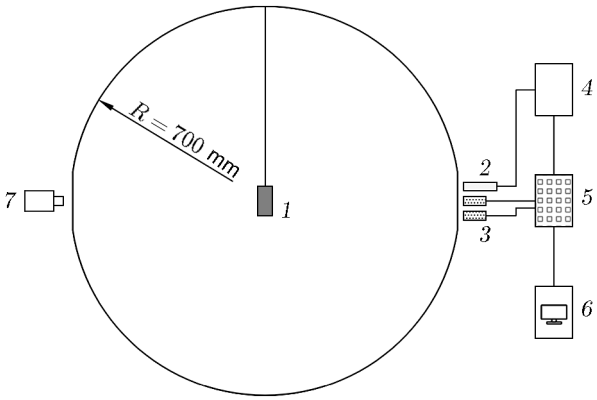

Fig. 2. Schematic of the explosion chamber (side view): (*1*) explosive charge; (*2*) fiber optic sensor; (*3*) PCB pressure gauges; (*4*) photoelectric converter; (*5*) data acquisition instrument; (*6*) computer; (*7*) high-speed camera.

The experiments were performed in a confined spherical explosion chamber with a volume of 1.43 m^3 schematically shown in Fig. 2. The chamber, which had a good seal and heat preservation, was made of steel. The chamber was provided with two flanges. Small equipment, such as gauges and bullet-proof glass, was installed on these flanges. In this work, a high-speed camera was used to record the growth of the fireball. The sampling frequency of the high-speed camera was set to 7000 frames per second. Two PCB pressure gauges and one fiber optic sensor were installed on the other flange. The pressure signals and optical signals during the explosion were obtained by a data acquisition instrument, whose sampling frequency was set at 1 MHz.

Before the test, air was removed from the chamber by using a vacuum system. Then, nitrogen (99.99%), dry air (containing 21% of oxygen), and oxygen (50% of oxygen + 50% of dry air) were introduced, and the pressure was kept consistent with the external environment (1 atm). As the test system and the vacuum system were not absolutely sealed, the maximum vacuum in the chamber could only reach 90% of the atmospheric value (90 kPa). Therefore, there were small amounts of other gases in the chamber, such as CO_2 and H_2O. However, the impact of these gases on the explosion was minimal. The charge was suspended from the center of the chamber and detonated by an electric detonator. Three parallel tests were performed for each formulation under the same test conditions. It should be noted that the laboratory was kept dark when the high-speed camera was working to avoid interference from ambient light.

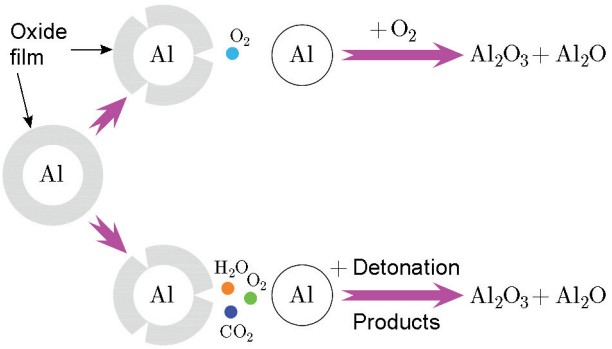

Fig. 3. Combustion reaction of the aluminum powder.

RESULTS AND ANALYSIS

When the aluminized explosive was detonated, chemical reactions of the components began. The aluminum particles were mainly oxidized to Al_2O_3 [16, 19], which radiated light signals to the ambient medium. Based on the assumption of a continuous spectrum of condensed-phase Al_2O_3 [20], an optical-electrical system was established. During the explosion, the optical signal was transmitted to the optical-electrical system via a PCS multicore quartz fiber optic sensor. Then, the optical signal was split and filtered, and the wavelength of the filter was set at 700 nm. The optical signal was then converted to a corresponding voltage signal by a photomultiplier tube and a photoelectric converter. Finally, the voltage signal was recorded by a data acquisition instrument with a sampling frequency of 1 MHz. The optical-electrical system was described in detail in a previously published paper [21].

Vaporized aluminum particles escaped from the ruptured oxide film during the explosion. The aluminum particles were rapidly oxidized to Al_2O_3 when they were exposed to oxygen and detonation products in the environment. The oxidation reaction and the main oxide of the aluminum particles are shown in Fig. 3. In addition, lower oxides (Al_2O_3, etc.) were also converted to Al_2O_3.

Herein, the voltage signal corresponds to an optical signal radiated by Al_2O_3. Therefore, the magnitude and timing of the voltage are closely related to the intense burning and duration of combustion. A typical voltage curve U as a function of time for TBX-A2 in different gas environments is shown in Fig. 4. It is seen that the voltage increases rapidly with t, then it decreases and finally returns to zero after a slight fluctuation above the baseline. However, the TBX-A2 voltage peaks and the duration of light emission are significantly different.

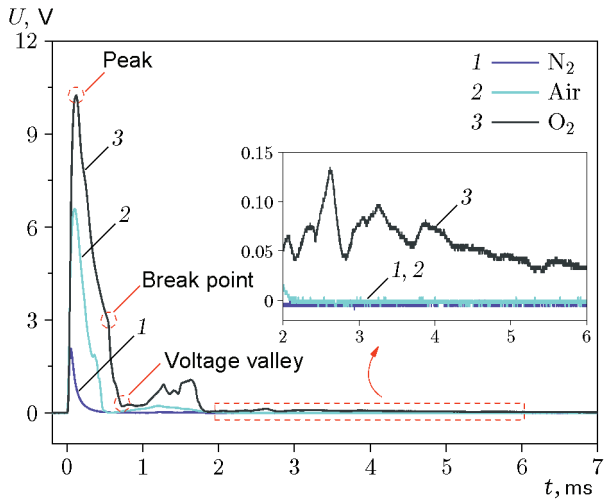

Fig. 4. Typical voltage-time curves for TBX-A2 in different gas environments.

According to the theory of afterburning reactions, it was determined that the test results were in line with what was expected. Therefore, the voltage-time curve $U(t)$ was divided into three stages denoted as I, II, and III with their respective voltage peaks and voltage valleys. The voltage peaks and the duration of light emission for each stage are listed in Table 2.

Stage I was the period when the voltage increased. Rapid mixing of the aluminum particles with the diffused detonation products occurred during the explosion. Oxygen in the environment was involved into the explosion field due to the effects of turbulence, but there was little oxygen entrapped. As shown in Fig. 4 and Table 2, when the fiber optic sensor received the optical signal of Al_2O_3, the voltages of all three rose sharply. This fact illustrated that the aluminum particles burned very quickly once they started to react. Moreover, the intense burning of aluminum particles could reach the maximum value in a short period of time. It could also be observed that the voltage peak for N_2 was the smallest one, with a value of only 21% of that of the O_2 peak. At the same time, the voltage of the former peaked nearly 40% faster than those of the other two. This means that the oxygen-poor environment limited the intense burning of the aluminum particles.

Stage II was the period when the voltage decreased. The aluminum particles were thoroughly mixed with oxygen and detonation products due to reflection of the blast wave. During this period, the aluminum particles continued to burn, while they were also rapidly consumed. After the majority of the aluminum particles were oxidized by O_2, the small amount remaining began to react with CO_2 and H_2O. This might be the cause of a break point in the voltage curve in the cases with air and O_2. In the N_2 environment, the voltage was rapidly reduced due to a low oxygen content, and this phenomenon was not present. According to Table 2, similar to the trend of stage I, the duration of stage II was prolonged as the oxygen content in the chamber increased. Stages I and II were the main periods in which aluminum particles burned, and their total time could reach hundreds of microseconds. By summing the time of these two stages, it was found that the burning time of the aluminum particles in air was 92.5% of that in O_2. In addition, the curve for O_2 shows that fluctuations in voltage were recorded after stage II. This means that the fraction of the aluminum particles that were only oxidized in air was smaller than 92.5%. It was stated earlier that the oxygen content in air was not sufficient to support the complete combustion of the aluminum particles.

Stage III was the period when the voltage oscillated. After the voltage valley, the voltage in air and O_2 still showed slight fluctuations. It might be that a very small number of the aluminum particles at the edge of the explosion field continued to burn. Another option was the oxidation reaction between the aluminum particles and certain intermediates. At the same time, this stage might be accompanied by a small amount of low-level aluminum oxides (Al_2O, etc.) being converted to Al_2O. Table 2 shows that stage III will continue for a long time in an oxygen-rich atmosphere. However, the energy released during this conversion period to Al_2O was inefficient for enhancing the explosion.

Intense burning can further increase the amount of active aluminum particles. The voltage value reflects the intense burning of the aluminum particles, and the voltage peak represents the maximum value that the energy release can reach in an instant. It is beneficial to increase the temperature of the fireball and maintain the continued transmission of the blast wave. The voltage peaks of four formulations in different gas environments are shown in Fig. 5. As the oxygen content in the chamber increases, the voltage peak gradually increases. Additionally, the voltage peaks of four formulations in O_2 increase by more than 130% compared to those in the air environment. It is also found that the voltage peaks in O_2 are similar except for TBX-A4. This illustrates that the energy release could immediately reach the maximum in the presence of a sufficient oxygen concentration, which almost negates the effect of the aluminum particle size. However, in air, this advantage was more pronounced for 23.8-μm aluminum particles. TBX-A1 and TBX-A2 have lower voltage peaks, which might also be caused by their lower content of active aluminum. Furthermore, the peak voltage for TBX-A4 is lower than those of the other three, indi-

Table 2. Voltage peaks and duration of light emission for TBX-A2 in different gas environments

Gas environment	Time, ms				Voltage peak, V
	Stage I	Stage II	Stage III	Total time	
N_2	0.049	0.446	0.203	0.698	2.125
Air	0.104	0.565	1.413	2.082	6.631
O_2	0.115	0.608	6.008	6.731	10.281

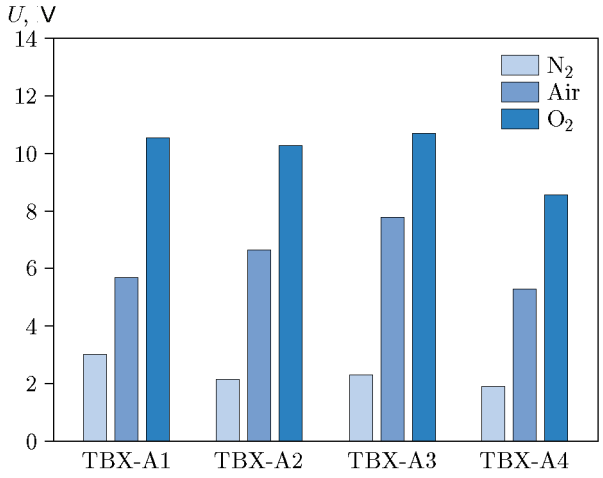

Fig. 5. Voltage peaks in different gas environments.

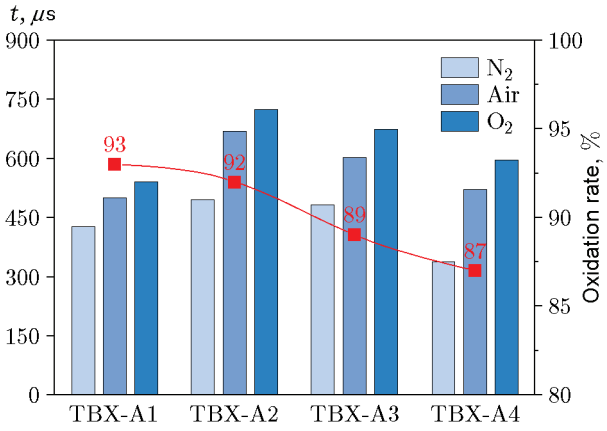

Fig. 6. Oxidation rate and duration of light emission in different gas environments.

cating that the release of the combustion energy from large-sized aluminum particles is limited. This means that the combustion conditions of large-sized aluminum particles are more stringent, which might be related to their smaller specific surface area.

The duration of light emission and the oxidation rate in different atmospheres are shown in Fig. 6. As the combustion of the aluminum particles was mainly concentrated at stages I and II, the time of these two stages was summed as the duration. Furthermore, the oxidation rate of the aluminum particles was the ratio of their durations in the air and O_2 environments. Figure 6 shows that the optical radiation signal of Al_2O_3 was recorded in the N_2 environment and lasted for hundreds of microseconds. Even a small amount of air remaining in the chamber could explain why some aluminum particles were oxidized with the detonation products with the formation of Al_2O_3. In addition, the possibility of aluminum particles reacting with nitrogen should also be taken into account. By comparing the duration in air and O_2, it is known that all four particle sizes of the aluminum particles were not completely oxidized in the air environment. It could be seen in Fig. 6 that the estimated oxidation rate of the aluminum particles was 87–93%. Moreover, as the size of the aluminum particles increases, the oxidation rate tends to decrease. This indicates that large aluminum particles were not conducive to the afterburning reaction. The reason for this difference might be that the surface of the large-sized aluminum particles had a thicker oxide film. This oxide film extended the heating time of the aluminum particles, resulting in an ignition delay and a smaller burning rate of active aluminum [22]. Taken together, small aluminum particles (5.4 μm) were more conducive to the afterburning reaction.

The further damage to the target by the fireball is a form of the thermal effect of the aluminized explosive. Therefore, the duration of the fireball is an important parameter for evaluating the explosion performance. A high-speed camera was used to record the features and global shape of the fireball to obtain the duration. A typical fireball of TBX-A2 in air is shown in Fig. 7. It can be clearly seen that the fireball has a distinct characteristic of light and dark regions. It should be noted that there were minor damages to the glass during the explosion, and these small black spots were negligible. When the grain was detonated, the fireballs in the visible area were all bright white light because of HMX detonation and intense burning of the aluminum particles. Then, as the aluminum particles were contin-

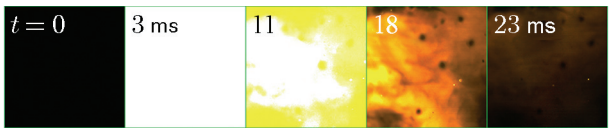

Fig. 7. Typical features and global shape of the TBX-A2 fireball in air.

uously consumed, the total energy slowly decreased. In this case, the white light in the area gradually turned yellow, and the color gradually became darker. During this period, a few residual aluminum particles were still oxidized, but the effect on increasing the total energy was very weak. After the end of the afterburning reaction, the fireball quickly extinguished and disappeared. Compared to the light emission of Al_2O_3, the duration of the fireball was very long and reached tens of milliseconds. This meant that the high-temperature state of the fireball could be maintained for a long time because there was a large amount of energy from the afterburning reaction. The heat loss of the fireball due to heat transfer was very slow and small relative to the total energy.

The fireball durations of the four formulations in different gas environments are shown in Fig. 8. It is clear that the fireball duration in the N_2 environment was minimal compared to that in air and oxygen, especially for TBX-A4, which lasted for only 6% of the duration of TBX-A1. It also shows that the oxidation reaction of 46.7-μm aluminum particles was highly dependent on oxygen. In addition, the degree of the reaction between the large-sized aluminum particles and detonation products was small. Comparing the duration of the fireball in air and O_2, it could be seen that the former was slightly smaller than the latter, and the aluminum particles were not completely burned. TBX-A1 had the shortest duration, which might be related to the greater burning rate of the nano-scale aluminum particles. Moreover, the low content of active aluminum also reduced the energy contributed by the combustion of the aluminum particles to the fireball. The duration increased first and then decreased as the particle size increased. This means that small micron-sized aluminum particles could extend the duration of the fireball, thereby extending the duration of the thermal effect and causing damage to the target for a longer time.

The primary pressure of the blast wave is mainly related to the initial energy of the explosion, that is, the energy of the detonation and the anaerobic combustion of the aluminized explosive. During detonation, the velocity of the primary blast wave was greater than that of the fireball; thus, the primary blast wave separated from the fireball. After that, the energy released from the afterburning reaction no longer enhanced the initial energy. It is well known that it is very difficult to measure the initial energy of an explosion. Therefore, this paper attempts to use the time difference between sensing the initial light and pressure wave arrival as a new method to describe the initial energy. During the explosion, the fiber optic sensor and the pressure sensor receive the corresponding signals, and there is a time difference between the light and pressure.

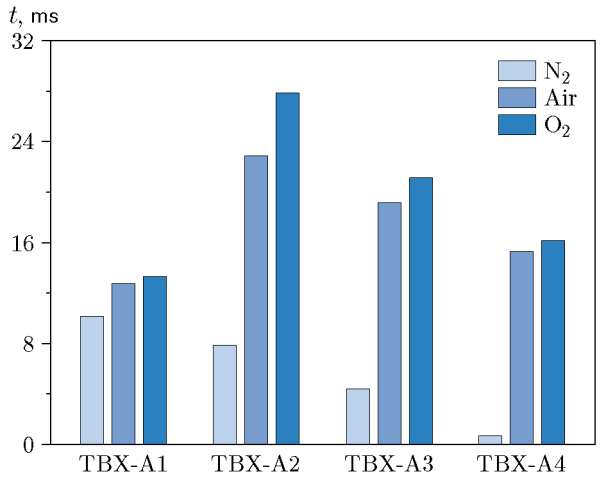

Fig. 8. Fireball duration in different gas environments.

After the charge suspended at the center of the chamber was detonated, the blast wave expanded and spread outward. At the same time, or perhaps even earlier, the aluminum particles were oxidized to Al_2O_3 and radiated light. In this chamber with a radius of 700 mm, the time it took for the optical signal to travel from the center to the fiber optic sensor was almost negligible. In comparison to the light, the propagation time of the blast wave in the gas mixture became very long. Therefore, when the fiber optic sensor received an optical signal, the primary blast wave was still propagating outward. The time difference between the optical signal and blast wave arrival could be approximated as the propagation time of the primary blast wave in the explosion field. However, the time difference was small, and it was inversely proportional to the initial energy.

The positions of the sensors were not changed during the test. Additionally, the changes in the medium of the explosion field were ignored. The light and pressure signals of each formulation in air are shown in Fig. 9, which illustrates that the time difference could reach up to hundreds of microseconds. Figure 10 shows the time difference in different gas environments, which tends to decrease with increasing oxygen content. This paper assumed that the afterburning reaction was lagging. Then, in the case where only the detonation provided energy, the time difference of each charge in the same gas environment should be approximately equal. Obvi-

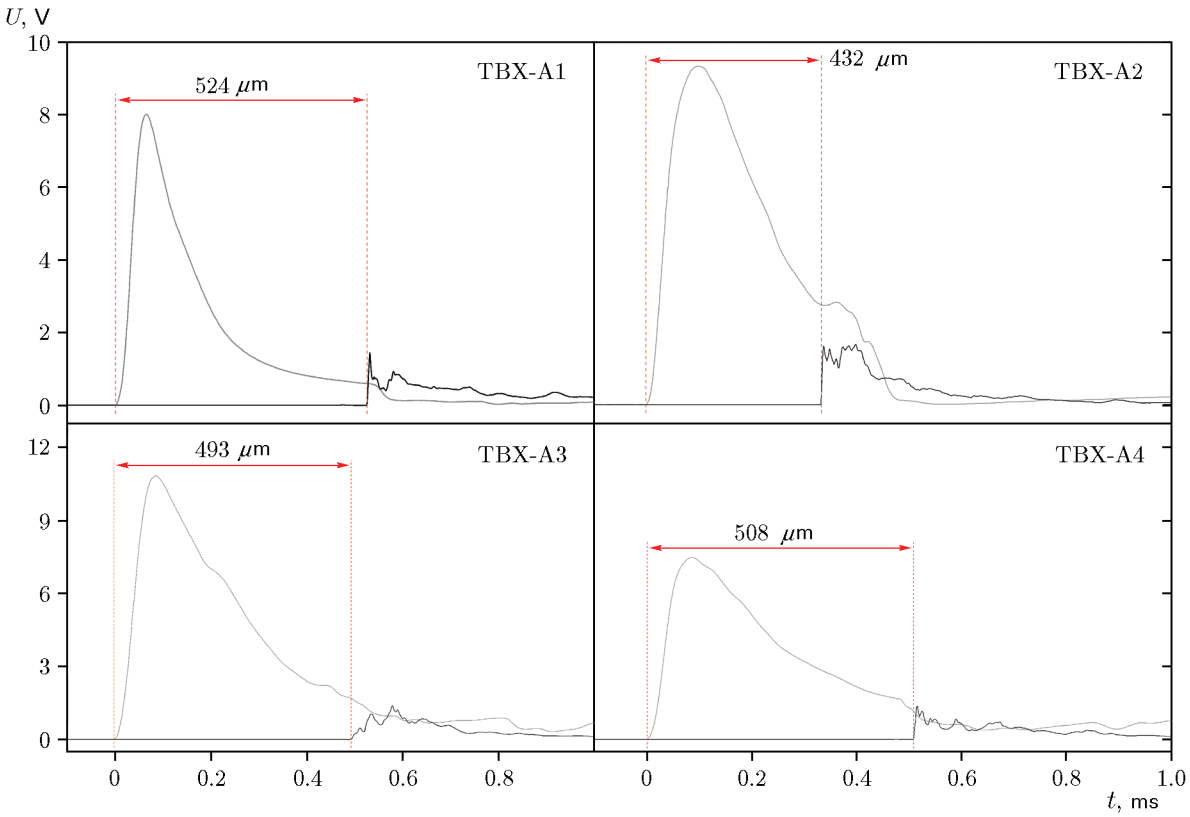

Fig. 9. Light and pressure signals of each formulation in air.

ously, it does not match the information given in Fig. 10. The results show that some of the aluminum particles were oxidized during the detonation and provided additional energy to the primary blast wave. Then, the velocity of the primary blast wave in the medium was changed, thereby affecting the time difference. Thus, the time difference first decreases and then increases as the size of the aluminum particles increases.

Figure 9 shows that the time difference for TBX-A2 in air was the smallest (432 μs), while that of TBX-A1 was the largest (524 μs), which was 121% of that of the former. According to the energy conservation law, the energy has a linear relationship with the squared velocity. Thus, it could be estimated that the initial energy of TBX-A2 was 11% higher than that of TBX-A1. The reliability of this estimate requires further verification because the amount of the aluminum particles participating in the oxidation reaction during the detonation is difficult to determine. In this case, however, a trend could still be extracted: small micron-sized aluminum particles have the advantage for increasing the initial energy.

The effect of the blast wave on the damage to the target is obvious, and the overpressure peak is an important parameter reflecting the explosion performance. The overpressure peaks of the four formulations in different gas environments are shown in Fig. 11. Although there were deviations in the measurement of pressure, some information could be extracted. Comparing the overpressure peaks in air and in N_2, the former was

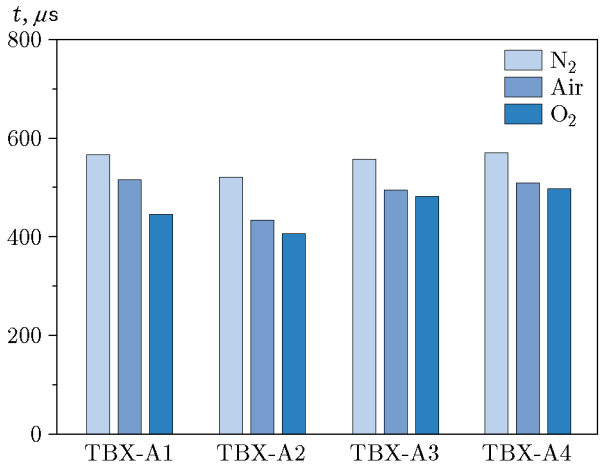

Fig. 10. Time difference between sensing the initial light and the pressure wave in different gas environments.

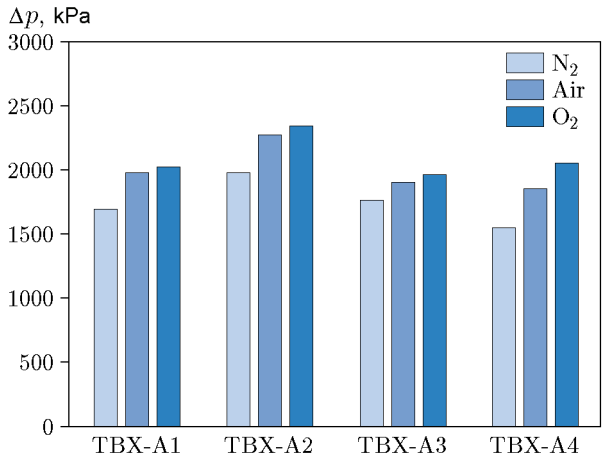

Fig. 11. Overpressure peaks of the examined explosive formulations in different gas environments.

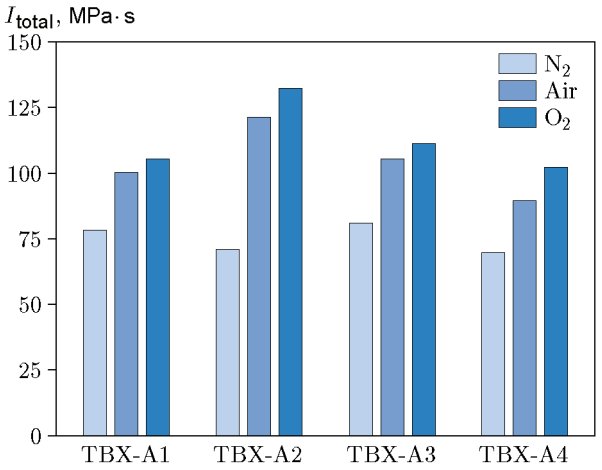

Fig. 12. Total impulse in different gas environments.

significantly larger than the latter. This indicated that the aluminum particles contributed to the enhancement of the primary pressure. As the oxygen content in the chamber increased, the overpressure peaks showed an increasing trend. However, except for TBX-A4, the trend was not obvious. This was probably because the oxidation reaction of the aluminum particles was close to saturation. The TBX-A4 charge with large-sized aluminum particles appeared to have a greater need for oxygen. In general, the overpressure peaks of TBX-A1, TBX-A3, and TBX-A4 were similar and lower than that of TBX-A2. It shows that the advantage of nano-aluminum was interrupted and reduced by the low content of active aluminum. This meant that 5.4-μm aluminum particles had the advantage for increasing the primary pressure.

In this paper, the total energy of the explosion is analyzed by the total impulse of the blast wave in a certain period. The attenuation of the total energy is primarily related to the chemical reaction and heat transfer. By using the same chamber, this paper assumes that the heat transfer and other heat losses for charges with equal masses during the explosion are the same. Thus, the attenuation of the total energy can be simplified to be related only to the afterburning reaction.

The total impulse I_{total} of the four kinds of charges in different gas environments is shown in Fig. 12. It is seen that the total impulse in nitrogen was lower than the other impulses, indicating that the energy released by the reaction of the detonation product with the aluminum particles in the oxygen-poor environment was small. If the oxygen content in the explosion field was sufficient, the afterburning reaction released as much energy as possible to maintain the continued propagation of the blast wave. It follows from the results of the total impulse in air and oxygen that the total impulse tended to increase first and then to decrease as the size of the aluminum particles increased. Compared to nano-aluminum, micron-sized aluminum particles with a higher content of active aluminum produced a significant effect on increasing their total impulse. Thus, the afterburning reaction provided an increase in additional energy for the explosion. This meant that small micron-sized aluminum particles more easily escaped from the oxide film and were oxidized or that the aluminum particles were more likely to be thrown into an oxygen-rich environment, thereby increasing the rate of combustion. The present study shows that comprehensive consideration of the particle size and the content of active aluminum can enhance the energy of aluminized explosives.

CONCLUSIONS

Based on the confined explosion of aluminized explosives in this study, it was found that the particle size and oxygen content play an important role in the afterburning reaction and explosion performance. After the analysis, the following conclusions were drawn.

1. The oxygen content in air is not sufficient to support the complete oxidation of aluminum particles. The estimated oxidation rate of aluminum particles is 87–93%, and the experimental values are actually smaller than this estimate. As the size of aluminum particles increases, the oxidation rate tends to decrease.

2. An oxygen-poor environment limits the intense burning of aluminum particles. Some of the aluminum particles oxidize with the detonation products to form Al_2O_3, and the reaction lasts for hundreds of microseconds. In addition, the degree of oxidation of large-sized aluminum particles with the detonation products is small.

3. Estimating the initial energy of the explosion by sensing the time difference between the initial light and the pressure wave is a feasible new method. This method led to a conclusion that some of the aluminum particles are oxidized during the detonation and provide additional energy to the primary blast wave.

4. Fireballs last up to tens of milliseconds. Small micron-sized aluminum particles in the range of 48.9 nm–46.7 μm extend the fireball duration. Moreover, it has a certain effect that promotes enhancement of the initial energy, overpressure peak, and total impulse.

The authors are thankful to Kun Chen, Mingfu Yang, and Hongwei Li for helping with the explosion tests in this work. Additional thanks to Xiaowen Hong for helping with the revision of this paper. The experimental instruments and equipment are also described in another paper to be published (External Review).

REFERENCES

1. J. R. Carney, J. M. Lightstone, T. P. McGrath II, and R. J. Lee, "Fuel-Rich Explosive Energy Release: Oxidizer Concentration Dependence," Propell., Explos., Pyrotech. **34** (4), 331–339 (2009).
2. K. L. McNesby, B. E. Homan, J. J. Ritter, et al., "Afterburn Ignition Delay and Shock Augmentation in Fuel Rich Solid Explosives," Propell., Explos., Pyrotech. **35**, 57–65 (2010).
3. W. A. Trzciński and J. Paszula, "Confined Explosions of High Explosives," J. Tech. Phys. **41** (4), 453–470 (2000).
4. P. P. Vadhe, R. B. Pawar, R. K. Sinha, et al., "Cast Aluminized Explosives (Review)," Fiz. Goreniya Vzryva 44 (4), 98–115 (2008) [Combust., Expl., Shock Waves **44** (4), 461–477 (2008)].
5. P. J. Haskins, M. D. Cook, and R. I. Briggs, "The Effect of Additives on the Detonation Characteristics of a Liquid Explosive," in *Proc. 12th APS Topical Group Meeting on Shock Compression of Condensed Matter, Atlanta, 2001*, pp. 890–893.
6. M. A. Trunov, M. Schoenitz, X. Y. Zhu, and E. L. Dreizin, "Effect of Polymorphic Phase Transformations in Al_2O_3 Film on Oxidation Kinetics of Aluminum Powders," Combust. Flame **140**, 310–318 (2005).
7. V. I. Levitas, "Burn Time of Aluminum Nanoparticles: Strong Effect of the Heating Rate and Melt-Dispersion Mechanism," Combust. Flame **156** (2), 543–546 (2009).
8. J. M. Peuker, H. Krier, and N. Glumac, "Particle Size and Gas Environment Effects on Blast and Overpressure Enhancement in Aluminized Explosives," Proc. Combust. Inst. **34**, 2205–2212 (2013).
9. W. K. Lewis, C. G. Rumchik, P. B. Broughton, and C. M. Lindsay, "Time-Resolved Spectroscopic Studies of Aluminized Explosives: Chemical Dynamics and Apparent Temperatures," J. Appl. Phys. **111**, 014903 (2012).
10. V. Tanguay, S. Goroshin, A. J. Higgins, and F. Zhang, "Aluminum Particle Combustion in High-Speed Detonation Products," Combust. Sci. Technol. **181**, 670–693 (2009).
11. T. Bazyn, H. Krier, and N. Glumac, "Evidence for the Transition from the Diffusion-Limit in Aluminum Particle Combustion," Proc. Combust. Inst. **31**, 2021–2028 (2007).
12. K. Park, D. Lee, A. Rai, et al., "Size-Resolved Kinetic Measurements of Aluminum Nanoparticle Oxidation with Single Particle Mass Spectrometry," Phys. Chem. B **109**, 7290–7299 (2005).
13. W. A. Trzciński, S. Cudziło, J. Paszula, and J. Callaway, "Study of the Effect of Additive Particle Size on Non-Ideal Explosive Performance," Propell., Explos., Pyrotech. **33** (3), 227–235 (2008).
14. L. Maiz, W. A. Trzciński, and J. Paszula, "Investigation of Fireball Temperatures in Confined Thermobaric Explosions," Propell., Explos., Pyrotech. **42** (2), 142–148 (2017).
15. K. Chen, W. Xiao, Z. W. Han, et al., "Effect of Aluminum Particle Size on the Explosion Parameters of HMX-Based Thermobaric Explosives in Confined Space," Chin. J. Explos. Propell. (2020); DOI: 10.14077/j.issn.1007-7812.201909018.
16. L. Maiz, W. A. Trzciński, M. Szala, and J. Paszula, "Studies of Confined Explosions of Composite Explosives and Layered Charges," Cent. Eur. J. Energ. Mater. **13**, 957–977 (2016).
17. L. Maiz, W. A. Trzciński, and M. Szala, "Preparation and Testing of Thermobaric Composites," in *Proc. 18th Seminar on New Trends in Research of Energetic Materials* (Pardubice, Czech Republic, 2015), pp. 705–715.
18. A. Rai, K. Park, L. Zhou, and M. R. Zachariah, "Understanding the Mechanism of Aluminum Nanoparticle Oxidation," Combust. Theory Modell. **10** (5), 843–859 (2006).
19. W. A. Trzciński, K. Barcz, J. Paszula, and S. Cudziło, "Investigation of Blast Performance and Solid Residues for Layered Thermobaric Charges," Propell., Explos., Pyrotech. **39**, 40–50 (2014).
20. S. Goroshin, J. Mamen, A. Higgins, et al., "Emission Spectroscopy of Flame Fronts in Aluminum Suspensions," Proc. Combust. Inst. **31**, 2011–2019 (2007).
21. J. B. Deng, *Study of the Damage Effects of Four Thermobaric Explosives* (Nanjing University of Science & Technology, 2013) [In chinese].
22. N. H. Yen and L. Y. Wang, "Reactive Metals in Explosives," Propell., Explos., Pyrotech. **37**, 143–155 (2012).